

# High-Resolution X-ray Study of Deoxyhemoglobin Rothschild 37 $\beta$ Trp $\rightarrow$ Arg: A Mutation That Creates an Intersubunit Chloride-Binding Site<sup>†,‡</sup>

Jeffrey S. Kavanaugh,<sup>§</sup> Paul H. Rogers,<sup>§</sup> David A. Case,<sup>||</sup> and Arthur Arnone<sup>\*,§</sup>

Department of Biochemistry, The University of Iowa, Iowa City, Iowa 52242, and Department of Molecular Biology, Research Institute of Scripps Clinic, La Jolla, California 92037

Received September 24, 1991; Revised Manuscript Received February 7, 1992

**ABSTRACT:** The mutation site in hemoglobin Rothschild (37 $\beta$  Trp  $\rightarrow$  Arg) is located in the "hinge region" of the  $\alpha 1\beta 2$  interface, a region that is critical for normal hemoglobin function. The mutation results in greatly reduced cooperativity and an oxygen affinity similar to that of hemoglobin A [Gacon, G., Belkhdja, O., Wajcman, H., & Labie, D. (1977) *FEBS Lett.* 82, 243-246]. Crystals were grown under "low-salt" conditions [100 mM Cl<sup>-</sup> in 10 mM phosphate buffer at pH 7.0 with poly(ethylene glycol) as a precipitating agent]. The crystal structure of deoxyhemoglobin Rothschild and the isomorphous crystal structure of deoxyhemoglobin A were refined at resolutions of 2.0 and 1.9 Å, respectively. The mutation-induced structural changes were partitioned into components of (1) tetramer rotation, (2) quaternary structure rearrangement, and (3) deformations of tertiary structure. The quaternary change involves a 1° rotation of the  $\alpha$  subunit about the "switch region" of the  $\alpha 1\beta 2$  interface. The tertiary changes are confined to residues at the  $\alpha 1\beta 2$  interface, with the largest shifts ( $\sim 0.4$  Å) located across the interface from the mutation site at the  $\alpha$  subunit FG corner-G helix boundary. Most surprising was the identification of a mutation-generated anion-binding site in the  $\alpha 1\beta 2$  interface. Chloride binds at this site as a counterion for Arg 37 $\beta$ . The requirement of a counterion implies that the solution properties of hemoglobin Rothschild, in particular the dimer-tetramer equilibrium, should be very dependent upon the concentration and type of anions present.

The  $\alpha_2\beta_2$  hemoglobin tetramer is characterized by pseudo-222 symmetry that gives rise to six subunit interfaces with different relative stabilities (Perutz, 1970; Ip & Ackers, 1977; Valdes & Ackers, 1977; Baldwin & Chothia, 1979). The least stable of these, the  $\alpha 1\alpha 2$  and  $\beta 1\beta 2$  interfaces, form a solvent channel that runs the length of the tetramer. The  $\alpha 1\beta 1$  (and symmetry-related  $\alpha 2\beta 2$ ) interface is the most stable interface. It is responsible for the formation of  $\alpha\beta$  dimers, and its stereochemistry does not change as a result of the T to R (i.e., the deoxy to oxy) quaternary transition. In contrast, the atomic interactions that constitute the  $\alpha 1\beta 2$  (and symmetry-related  $\alpha 2\beta 1$ ) interface break when the tetramer dissociates into dimers, and they are sensitive to the quaternary structure of the tetramer. A wide range of studies, including X-ray crystallographic (Perutz, 1970; Baldwin & Chothia, 1979), thermodynamic (Pettigrew et al., 1982), and theoretical (Gelin & Karplus, 1977; Gelin et al., 1983), indicate that the oxygen-linked rearrangement of the  $\alpha 1\beta 2$  interface is an essential component of hemoglobin's cooperative mechanism.

In this paper, we report the high-resolution X-ray structure of deoxyhemoglobin Rothschild, a naturally occurring mutant hemoglobin that is characterized by the substitution of an arginine for a tryptophan at position 37 $\beta$  in the  $\alpha 1\beta 2$  interface (Gacon et al., 1977). Analysis of the mutation-induced structural changes provides a basis for understanding the functional consequences of the mutation: reduced cooperativity, an oxygen affinity that can be moderately higher or

moderately lower than that of hemoglobin A, and destabilization of both the deoxy and oxy tetramers (Gacon et al., 1977; Sharma et al., 1980; Doyle and Ackers, personal communication).

## MATERIALS AND METHODS

**Hemoglobin Preparation.** Purified deoxyhemoglobin Rothschild was a gift from Dr. Gary Ackers (Washington University, St. Louis, MO). Prior to crystallization, the mutant hemoglobin was dialyzed into 10 mM ammonium phosphate at pH 7.0. Native deoxyhemoglobin A was purified according to the procedure of Perutz (1968) from a fresh unit of blood drawn from a healthy nonsmoker. Both hemoglobins were stored frozen as pellets in liquid nitrogen until used for crystallization.

**Crystallization of Deoxyhemoglobin A and Deoxyhemoglobin Rothschild.** Crystals of deoxyhemoglobin A were grown at room temperature using the batch method previously described (Ward et al., 1975; Arnone et al., 1980). The best deoxyhemoglobin A crystals grew from solutions consisting of 10 mg/mL hemoglobin, 10 mM potassium phosphate (pH 7.0), 100 mM potassium chloride, 4 mM sodium dithionite, and 10-10.5% PEG<sup>1</sup> 6000.

Attempts to crystallize deoxyhemoglobin Rothschild from solutions of concentrated ammonium sulfate, as described by Perutz (1968) for deoxyhemoglobin A, failed to yield well-formed crystals. Crystals of deoxyhemoglobin Rothschild were obtained using PEG, as described above, with the addition of a seeding step. Specifically, a crystal of deoxyhemoglobin A was washed in a substitute mother liquor consisting of 10 mM potassium phosphate at pH 7.0, 100 mM potassium chloride, and 15% PEG. The crystal was then crushed in 200  $\mu$ L of 33.3% PEG (unbuffered). After the larger fragments of the

<sup>†</sup> This work was supported by grants from the National Institutes of Health (HL-40453 and GM-40852).

<sup>‡</sup> Crystallographic coordinates and structure factors have been submitted to the Brookhaven Protein Data Bank (deoxyhemoglobin Rothschild coordinates, 1HBA; deoxyhemoglobin A coordinates, 1HBB; deoxyhemoglobin Rothschild structure factors, R1HBASF; deoxyhemoglobin A structure factors, R1HBBSF).

<sup>§</sup> The University of Iowa.

<sup>||</sup> Research Institute of Scripps Clinic.

<sup>1</sup> Abbreviations: PEG, poly(ethylene glycol); rms, root mean square; Na<sub>2</sub>EDTA, disodium ethylenediaminetetraacetate.

Table I: Unit Cell Constants, Space Group  $P2_12_12_1$ <sup>a</sup>

hemoglobin	a (Å)	b (Å)	c (Å)
deoxyhemoglobin A	97.1	99.3	65.8
deoxyhemoglobin Rothschild	97.1	99.3	66.1
Br <sup>-</sup> soaked deoxyhemoglobin Rothschild	97.0	99.2	66.1

<sup>a</sup> The uncertainty in these measurements is about 0.1 Å.

crushed crystal had settled to the bottom of the vial, 2  $\mu$ L of this solution was used in place of 2  $\mu$ L of the stock PEG solution in 100- $\mu$ L deoxyhemoglobin Rothschild setups. This procedure yielded well-formed microcrystals of deoxyhemoglobin Rothschild within 2 days, with the best microcrystals growing in vials containing approximately 8.5% PEG. These microcrystals were washed in the substitute mother liquor described above and used as seeds (one seed per vial) in 125- $\mu$ L deoxyhemoglobin Rothschild setups. At PEG concentrations between 10.5% and 11.5%, these seeds grew into well-formed crystals that are isomorphous with crystals of deoxyhemoglobin A (Table I). A concentration of 8 mM sodium dithionite was used in the deoxyhemoglobin Rothschild batch setups as well as in all substitute mother liquors used during crystal manipulations. All crystallization stock solutions, substitute mother liquors, and hemoglobin solutions were thoroughly deoxygenated prior to their use, and all work was conducted in a nitrogen-filled glove box.

**Collection of Diffraction Data.** The deoxyhemoglobin A and deoxyhemoglobin Rothschild crystals were mounted in quartz capillaries. Diffraction data were collected on a single deoxyhemoglobin Rothschild crystal using the multiwire area detectors at The University of California at San Diego Resource for Protein Crystallography. A total of 33 303 unique reflections (101 776 total measurements) were collected, representing 77% of the possible data out to a resolution of 2.0 Å. The data are 92% complete out to a resolution of 2.15 Å and 10% complete in the 2.15–2.0-Å shell. The diffraction data are of high quality as judged by an  $R_{\text{symm}}$ <sup>2</sup> value of 4.3% on intensity for all data out to 2.0 Å.

Diffraction data were collected with a single deoxyhemoglobin A crystal on a Rigaku AFC6R diffractometer fitted with a San Diego Multiwire Systems area detector. A total of 185 171 measurements were made of 47 999 independent reflections. The data are 95% complete out to a resolution of 1.91 Å and have an  $R_{\text{symm}}$  of 4.4%. The data are 99% complete out to 2.05-Å resolution and 78% complete in the 2.05–1.91-Å shell. All diffraction data were scaled and merged according to the procedure of Howard et al. (1985).

**Identification of a New Anion-Binding Site in Deoxyhemoglobin Rothschild.** The presence of a new anion-binding site in  $\alpha 1\beta 2$  interface of deoxyhemoglobin Rothschild was confirmed by soaking a crystal in a substitute mother liquor consisting of 10 mM potassium phosphate at pH 7.0, 100 mM potassium bromide, 8 mM sodium dithionite, and 13.3% PEG. The crystal was washed twice with 0.5 mL of this solution and then soaked for 2 days in a third 0.5-mL aliquot. Diffraction data were collected to a resolution of 2.4 Å on the same diffractometer that was used to collect the deoxyhemoglobin A diffraction data. Soaking the crystal resulted in increased peak widths and diminished quality of the diffraction data as indicated by an  $R_{\text{symm}}$  of 11.4%. Nevertheless, a difference Fourier map, produced with  $|F_{\text{Br}^-\text{soak}} - F_{\text{Cl}}|$  magnitudes and calculated phases, clearly revealed the anion-binding site.

**Refinement Strategy.** The refinement of the deoxyhemoglobin Rothschild structure was carried out with the

restrained least-squares program PROLSQ of Hendrickson and Konnert (Hendrickson, 1985). The starting coordinates were those of a partially refined 2.5-Å deoxyhemoglobin A structure (Fantl et al., 1987). The general strategy employed during the refinement was to run successive PROLSQ cycles until convergence was reached, at which point Fourier maps were calculated and inspected using interactive computer graphics. Following manual rebuilding of the model, stereochemically restrained least-squares refinement was resumed. During the early manual interventions, deleted  $F_o - F_c$  Fourier maps, in which residues comprising approximately 6% of the total structure had been deleted, were used to make adjustments in side-chain positions and to rebuild areas of the model containing problems in main-chain positions or geometry. During the later stages of the refinement,  $F_o - F_c$  and  $2F_o - F_c$  maps were used to identify and add solvent molecules to the model. PROLSQ cycles were run on a VAX 6410, and Fourier maps were calculated on a VAX 3200. Interactive computer graphics sessions were conducted on a Silicon Graphics workstation using the program TOM/FRODO (Cambillau, 1989), a version of the program FRODO (Jones, 1985).

Comparison of the refined deoxyhemoglobin Rothschild atomic model with the deoxyhemoglobin A starting model showed relatively large atomic displacements at the mutation site, as well as smaller changes in the  $\alpha$  subunits at a distance from the mutation site. Specifically, overlaying the models indicated an apparent shift of the  $\alpha$  subunit F helix (which is across the  $\alpha 1\beta 2$  interface from the mutation at 37 $\beta$ ) away from the  $\alpha 1\beta 2$  interface. The smaller structural differences could have been mutation induced, or they simply could have resulted from the correction of model errors inherent in the initial 2.5-Å deoxyhemoglobin A structure. Therefore, it was decided to see if the same small changes could be detected (in reverse) by "back-refining" (with the PROLSQ program) the deoxyhemoglobin Rothschild atomic model against the new 1.9-Å deoxyhemoglobin A data set. In order to eliminate the possibility that the small structural changes were somehow dependent on the refinement program, the program XPLOR (Brünger et al., 1987) was also used to carry out a concurrent refinement of deoxyhemoglobin Rothschild, followed by a back-refinement of this model against the 1.9-Å deoxyhemoglobin A data set. The XPLOR refinements were conducted on a Convex computer and utilized the standard heating and cooling cycles and final temperature factor refinement suggested by Brünger et al. (1987).

**Superposition of Protein Structures.** Superpositions of the deoxyhemoglobin Rothschild and deoxyhemoglobin A structures were carried out using the method of Kabsch (1976) as implemented in the program BMFIT by S. C. Nyburg. In each case, the main-chain atoms were superimposed after omitting residues with temperature factors greater than 25 Å<sup>2</sup> (i.e., relatively mobile residues that are found at the corners between helices and at the NH<sub>2</sub> termini). In addition, portions of  $\alpha$  chain FG corner (residues 94 $\alpha$ –97 $\alpha$ ) and the  $\beta$  chain C helix (residues 35 $\beta$ –39 $\beta$ ) were deleted from the superpositions because "C $\alpha$   $\Delta$ -distance plots" (Kuriyan et al., 1986) indicated that these regions contained the largest perturbations in tertiary structure (data not shown). After excluding these residues, each  $\alpha$  chain contributed 388 of 564 main-chain atoms, and each  $\beta$  chain contributed 452 or 584 main-chain atoms to the least-squares superposition. By superimposing all four globin chains of the deoxyhemoglobin Rothschild on those the deoxyhemoglobin A, rigid-body rotation and translation of the tetramer can be separated from changes in quaternary and tertiary structure. Superimposing a single  $\alpha$  or  $\beta$  subunit of

<sup>2</sup>  $R_{\text{symm}} = \sum_{hkl} (|I_{hkl} - \bar{I}_{hkl}|) / \sum_{hkl} \bar{I}_{hkl}$

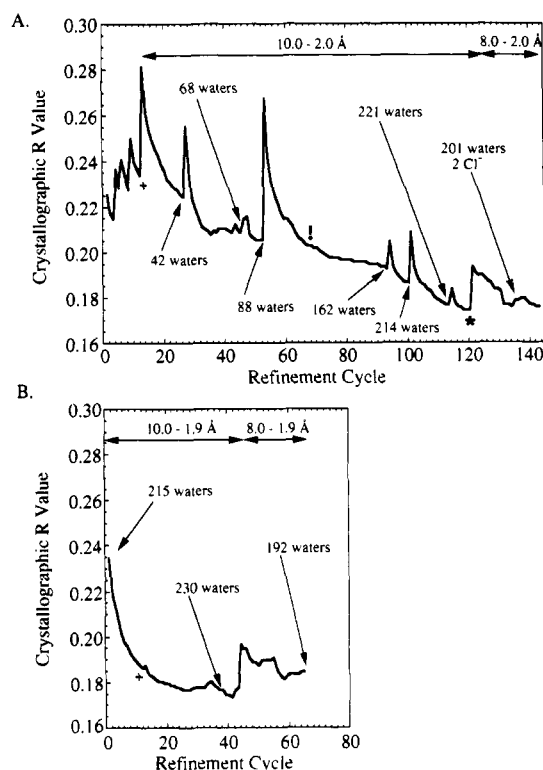


FIGURE 1: Courses of the PROLSQ deoxyhemoglobin Rothschild refinement and PROLSQ deoxyhemoglobin A back-refinement are plotted in panels A and B, respectively. The resolution limits are indicated at the top of each plot. The total number of solvent molecules in each model is indicated at various points in the refinements. The symbols denote the following: (+) the inclusion of the side chain atoms of 37 $\beta$  in the atomic model; (!) the initial model for the XPLOR refinement; and (\*) the initial model for the deoxyhemoglobin A back-refinement.

deoxyhemoglobin Rothschild on its deoxyhemoglobin A counterpart allows perturbations in tertiary structure to be separated from quaternary structure changes.

## RESULTS

**Refinement Results.** The course of the deoxyhemoglobin Rothschild refinement and the deoxyhemoglobin A back-refinement are charted in Figure 1. The starting model for the deoxyhemoglobin Rothschild refinement was constructed from the previously reported 2.5-Å model of human deoxyhemoglobin A (Fantl et al., 1987) by converting residue 37 $\beta$  to an alanine. During the first round of PROLSQ refinement, the resolution limits were increased in increments so that by cycle number 12 all of the deoxyhemoglobin Rothschild data between 10.0- and 2.0-Å resolution with magnitudes greater than  $4\sigma$  were included. The standard crystallographic  $R$  value<sup>3</sup> for this model, which contained no solvent, was 23.4%. At this point, the entire structure was inspected using deleted  $F_o - F_c$  Fourier maps. The arginine side-chain atoms were added to residue 37 $\beta$  (indicated by the "+" in Figure 1A), and manual adjustments of the model were made, primarily to the corners between helices. Refinement of this model against the Rothschild diffraction data lowered the  $R$  value to 22.5% by cycle number 25. The entire model was again inspected using deleted  $F_o - F_c$  Fourier maps, and a total of 42 water molecules were added. This lowered the  $R$  value to 20.9% by cycle 44. Following cycle number 44, four of the 42 water molecules were deleted and 30 new waters were added, bringing the total number of water molecules to 68. The large increase in the  $R$  value following the next manual rebuilding (after cycle 52)

was due in part to an attempt to reset many side-chain  $\chi$  angles closer to staggered, ideal values.

The atomic displacements in the  $\alpha$  chains, described above, were apparent when the cycle 66 Rothschild model (indicated by the exclamation point in Figure 1A) was compared to the initial deoxyhemoglobin A model. A trial back-refinement of the cycle 66 Rothschild model against the deoxyhemoglobin A diffraction data demonstrated the validity of the shifts. However, in order to characterize these structural changes more accurately, it was decided to carry out a full back-refinement after the deoxyhemoglobin Rothschild refinement was complete. The concurrent refinement of the Rothschild structure with the program XPLOR was initiated at this point, using the cycle 66 output as the initial model.

The remainder of the deoxyhemoglobin Rothschild refinement with PROLSQ consisted primarily of the systematic addition of more solvent molecules to the model. After cycle 92, waters were identified using a program, PEAKS, that searches a  $F_o - F_c$  Fourier map for peaks above a user-defined threshold. A second program, ANAL\_PEAKS, was used to identify which of these peaks were within proper hydrogen-bonding distance to the model. Water molecules were added to the model if the peak intensity was greater than 3 times the rms value of the  $F_o - F_c$  map and were retained in the final model if their temperature factor was  $70 \text{ Å}^2$  or less. The model resulting from cycle 119 (indicated by the asterisk in Figure 1A) contained 221 water molecules and had a  $R$  value of 17.6% for all  $4\sigma$  data between 10.0- and 2.0-Å resolution. This model was used as the starting point for the back-refinement against the 1.9-Å deoxyhemoglobin A data. Refinement cycles subsequent to cycle number 119 involved changes in resolution and intensity limits that affected the  $R$  value and the temperature factors for some water molecules but caused no substantial alterations of the protein model. Following refinement cycle 136, 12 water molecules were deleted because their temperature factors exceeded  $70 \text{ Å}^2$ . In addition, two water molecules were changed to chloride ions, one for the  $\alpha 1\beta 2$  interface and one for the  $\alpha 2\beta 1$  interface, on the basis of the results of the ( $\text{Br}^-$  vs  $\text{Cl}^-$ ) difference electron density map. Following the last refinement cycle (cycle 143), six additional water molecules were deleted due to temperature factors greater than  $70 \text{ Å}^2$ . The final deoxyhemoglobin Rothschild model has a standard crystallographic  $R$  value of 17.6% for all diffraction data between 8.0- and 2.0-Å resolution with magnitudes greater than  $2\sigma$  (30 741 reflections). The refinement statistics for the deoxyhemoglobin Rothschild model, as well as those for the deoxyhemoglobin A model, are reported in Table II.

The initial model for the deoxyhemoglobin A back-refinement was the Rothschild model output from cycle 119 in which the arginine at 37 $\beta$  was converted to an alanine. Six water molecules in close proximity to 37 $\beta$  were also deleted from the initial model. The  $R$  value for this model against the deoxyhemoglobin A diffraction data between 10.0- and 1.9-Å resolution and greater than  $4\sigma$  was 23.5%. The  $R$  value dropped to 18.4% by cycle 11, at which time the tryptophan side chains were added to the model using deleted  $F_o - F_c$  Fourier maps (indicated by the "+" in Figure 1B). After cycle 38, an additional 15 water molecules were added to the deoxyhemoglobin A model. The increase in  $R$  value following cycle 44 is the result of lowering the intensity criterion for including reflections in the refinement from  $4\sigma$  to  $2\sigma$ . Inspection of the model from the last refinement cycle revealed 38 water molecules with temperature factors greater than  $70 \text{ Å}^2$ . These water molecules were deleted from the final de-

<sup>3</sup>  $R$  value =  $\sum ||F_o| - |F_c|| / \sum |F_o|$ .

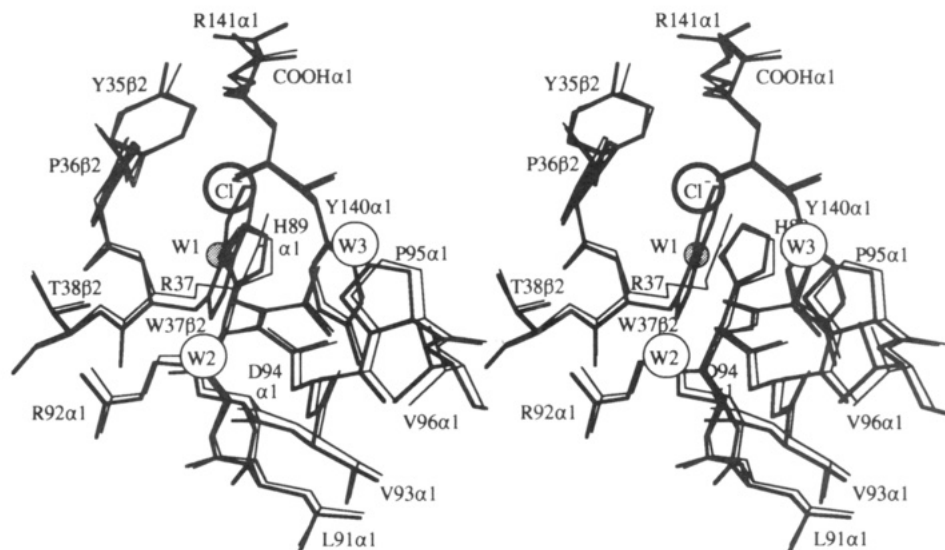


FIGURE 2: Stereodigram of the hemoglobin Rothschild mutation site at the  $\alpha 1\beta 2$  interface. Shown are  $\beta$  chain residues 34–38 and  $\alpha$  chain residues 88–96 and 140–141. (For clarity, the side chain of residue Lys 90 $\alpha$  has been omitted.) The deoxyhemoglobin Rothschild structure (thin bonds) is overlaid on the deoxyhemoglobin A structure (thick bonds), after the two tetramers were superimposed (see text). Water molecule W1 (filled circle) is part of the native interface, and water molecules W2 and W3 (labeled open circles) are part of the mutant interface. The chloride anion (circled Cl<sup>-</sup>) is associated with the mutant structure. The shift of the  $\alpha$  subunit FG corner and G helix away from the interface is largely due to deformations in tertiary structure, but a small portion of the shift is due to a rigid-body rotation of the  $\alpha$  subunit (see text).

Table II: Summary of Least-Squares Refinement Parameters (Hendrickson, 1985)

parameter	target $\sigma^a$	rms $\Delta^b$ deoxy Roths- schild	rms $\Delta^b$ deoxy HbA
bonding distances (Å)			
bond lengths (1–2 neighbors) <sup>c</sup>	0.010	0.011	0.010
1–3 neighbor distances <sup>d</sup>	0.015	0.025	0.024
1–4 planar neighbor distances <sup>e</sup>	0.030	0.042	0.040
planar groups			
deviations from plane (Å)	0.010	0.010	0.010
chiral centers			
chiral volumes (Å <sup>3</sup> )	0.080	0.131	0.130
nonbonded contacts (Å)			
separated by one torsion angle	0.200	0.165	0.161
all other van der Waals	0.200	0.182	0.177
contacts			
possible hydrogen bonds	0.200	0.174	0.159
conformational torsion angles (deg)			
planar (e.g., peptide $\omega$ )	5.0	2.5	2.2
staggered (e.g., aliphatic $\chi$ )	15.0	20.2	19.4
transverse (e.g., aromatic $\chi_2$ )	25.0	29.0	31.2
isotropic temperature factors (Å <sup>2</sup> )			
main chain (1–2 neighbors) <sup>c</sup>	1.5	1.9	1.8
main chain (1–3 neighbors) <sup>d</sup>	2.0	2.8	2.6
side chain (1–2 neighbors) <sup>c</sup>	4.0	6.9	6.8
side chain (1–3 neighbors) <sup>d</sup>	6.0	9.7	9.9

<sup>a</sup> Target  $\sigma$ , estimated standard deviations, where  $1/\sigma^2$  is used as a relative weighting factor in the minimized sum of observational functions. <sup>b</sup> rms  $\Delta$ , root-mean-square deviation from ideal values as determined from accurate small molecule crystal structures in the case of bonding distances, chiral volumes, and nonbonded contacts, or from average values in the case of isotropic temperature factors. <sup>c</sup> 1–2 neighbors, covalently bonded atom pairs. <sup>d</sup> 1–3 neighbors, atom pairs separated by two covalent bonds. <sup>e</sup> 1–4 planar neighbors, atom pairs in a planar group separated by three covalent bonds.

oxyhemoglobin A model, lowering the number of water molecules to 192. The deoxyhemoglobin A model has a standard crystallographic *R* value of 18.5% for all diffraction data between 8.0- and 1.9-Å resolution with magnitudes greater than  $2\sigma$  (44 919 reflections).

**Structural Changes at the  $\alpha 1\beta 2$  Interface.** The  $\alpha 1\beta 2$  interface exhibits pseudo 2-fold symmetry, a consequence of its

assembly from homologous portions of the  $\alpha$  and  $\beta$  chains. Using the terminology of Baldwin and Chothia (1979), the homologous portions of the  $\alpha 1\beta 2$  interface are referred to as the hinge and switch regions; residues from the  $\alpha 1$  C helix (36 $\alpha$ –43 $\alpha$ ) and the  $\beta 2$  FG corner and G helix (96 $\beta$ –103 $\beta$ ) interact to form the switch region, while residues from the  $\beta 2$  C helix (35 $\alpha$ –42 $\alpha$ ) and the  $\alpha 1$  FG corner and G helix (91 $\alpha$ –97 $\alpha$ ) form the hinge region. The Rothschild mutation, 37 $\beta$ -(C3) Trp  $\rightarrow$  Arg, occurs in the hinge region.

A stereoview of the mutation site is shown in Figure 2 where the main-chain atoms of the native and mutant tetramers have been superimposed. Figure 3 catalogues all the subunit–subunit interactions (contacts less than 3.5 Å) for the  $\alpha 1\beta 2$  interface in both of the PROLSQ-refined structures. From Figure 3 it is clear that the switch region is only slightly perturbed by the Rothschild mutation, whereas several intersubunit contacts are altered in the hinge region. In order to highlight these changes, the altered interactions are represented by dashed lines, the solvent molecules that differ between the two structures are indicated by numbered boxes rather than circles, and the anion in the mutant interface is represented as a triangle. That is, all the dashed lines in Figure 3A represent interactions that are lost, while those in Figure 3B represent new contacts that are gained, as a result of the Trp to Arg substitution. Although not shown in this paper, the counterparts to Figures 2 and 3 for the  $\alpha 2\beta 1$  interface in the PROLSQ-refined structures, as well as those for the  $\alpha 1\beta 2$  and  $\alpha 2\beta 1$  interfaces in the XPLOR-refined structures, show virtually identical results.

In deoxyhemoglobin A the indole nitrogen of Trp 37 $\beta$  is hydrogen bonded to the O<sub>δ1</sub> carboxyl oxygen of Asp 94 $\alpha$ , and the C<sub>3</sub> atom of the indole ring makes weak van der Waals contact with the side chain of Tyr 140 $\alpha$ . These interactions are replaced, in deoxyhemoglobin Rothschild, by a salt bridge that forms between the guanidinium atoms N<sub>ε</sub> and N<sub>η1</sub> of Arg 37 $\beta$  and the O<sub>δ1</sub> carboxyl oxygen of Asp 94 $\alpha$ . In addition, the mutation alters the arrangement of water molecules at the  $\alpha 1\beta 2$  interface and creates a new anion-binding site. Specifically, the water molecule labeled W1 forms a bridge across the  $\alpha 1\beta 2$  interface in deoxyhemoglobin A by hydrogen bonding to the main-chain N of Trp 37 $\beta$  and the carbonyl oxygens of

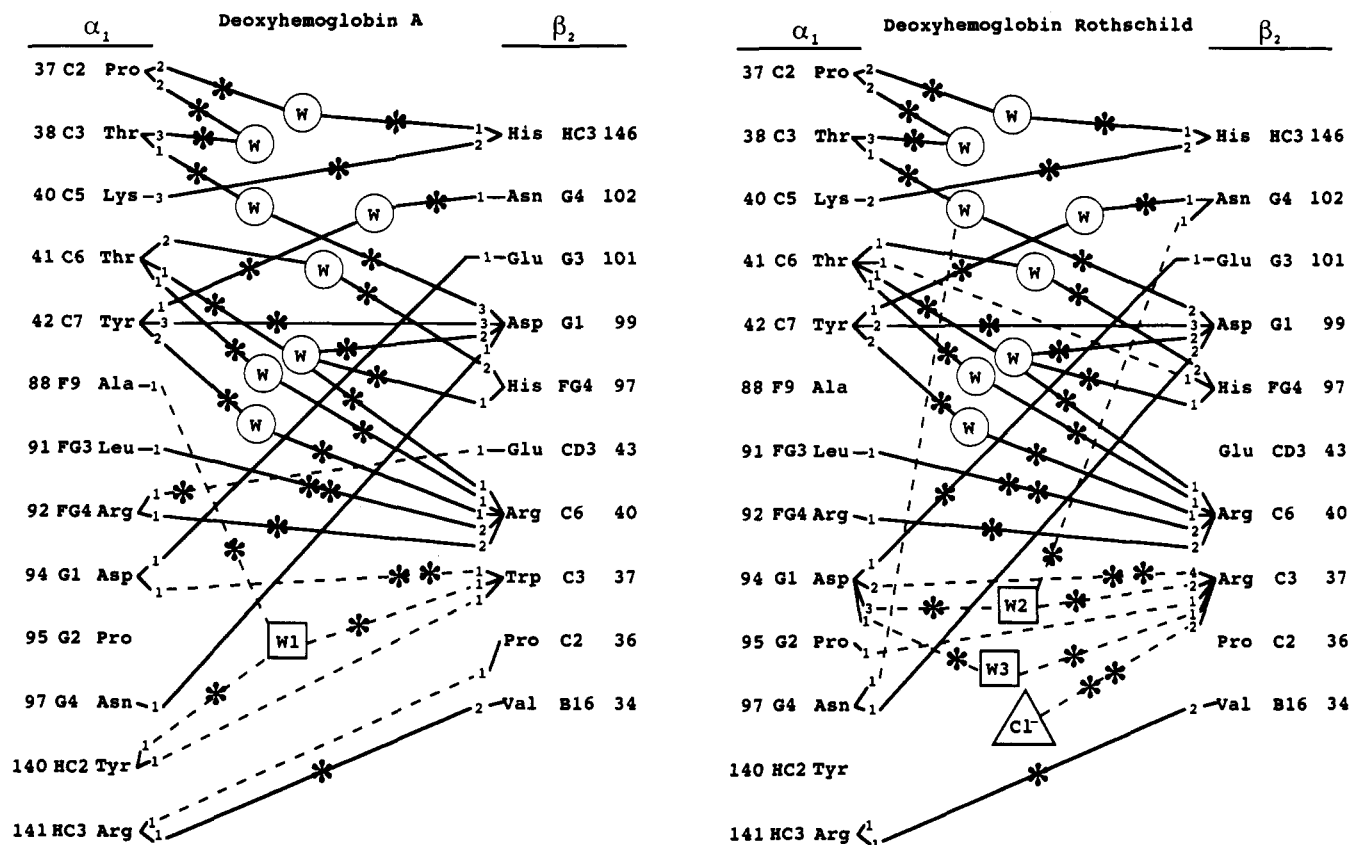


FIGURE 3: Intersubunit contacts at the  $\alpha_1\beta_2$  interface of deoxyhemoglobin A (left) and deoxyhemoglobin Rothschild (right). Each line connecting two residues represents an atomic interaction of 3.5 Å or less. The numbers found at the ends of each line are the number of atoms each residue contributes to the interaction. An ionic or polar interaction is marked by an asterisk. Interactions found in both the native and mutant interfaces are indicated by solid lines, and conserved water molecules are represented by a circled W. Contacts lost from the native interface and gained in the mutant interface are shown by dashed lines. Waters found in one interface, but not the other, are numbered and enclosed in squares. The chloride anion in the mutant structure is indicated by Cl<sup>-</sup>.

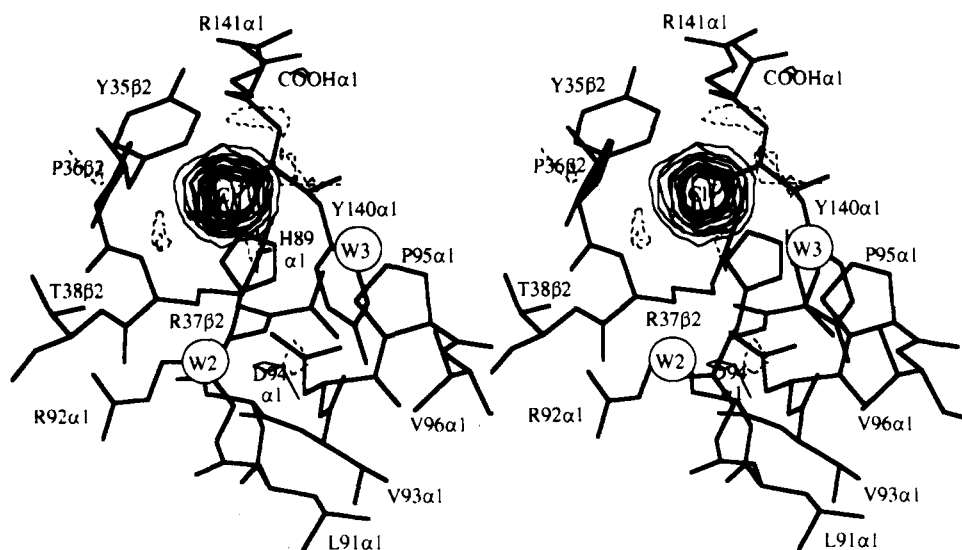


FIGURE 4: Stereodiagram of the  $\alpha_1\beta_2$  interface of deoxyhemoglobin Rothschild with the (Br-Cl<sup>-</sup>) difference Fourier map superimposed. Solid contours represent increases in electron density; dashed contours decrease in electron density. The contours are drawn in increments of 3 times the rms value of the difference map. The large positive peak reveals the anion-binding site between the guanidinium group of Arg 37 $\beta$  and the main-chain atoms of the same residue.

Ala 88 $\alpha$  and Tyr 140 $\alpha$ . In deoxyhemoglobin Rothschild, however, water W1 is absent and two new solvent sites are created. Water molecules W2 and W3 both bridge the interface by forming hydrogen bonds with the side chains of Arg 37 $\beta$  and Asp 94 $\alpha$ . Water molecule W2 extends the influence of the Trp to Arg substitution into the switch region of the  $\alpha_1\beta_2$  interface by making an additional hydrogen bond with Asn 102 $\beta$ .

The new anion-binding site (indicated by the Cl<sup>-</sup> in Figures 2, 3, and 4) is between the N<sub>72</sub> atom and the main-chain amide N of Arg 37 $\beta$ . The chloride ion in this site was initially modeled as a water molecule, but a very low temperature factor (5 Å<sup>2</sup> in one interface and 2 Å<sup>2</sup> in the other) made it suspect. Superimposing the (Br<sup>-</sup> vs Cl<sup>-</sup>) difference electron density map (see Materials and Methods) on the atomic model of the  $\alpha_1\beta_2$  interface (Figure 4) confirms the presence of a

chloride ion. The large positive peak (which is 32 times the rms density of the difference map) centered over the  $\text{Cl}^-$  is the only prominent feature of the difference map and corresponds to the difference between bromide (35 electrons) and chloride (17 electrons).  $\text{Cl}^-$  anions (one at the  $\alpha 1\beta 2$  interface and one at the  $\alpha 2\beta 1$  interface) were added to the atomic model for the last seven cycles of PROLSQ refinement. With the  $\text{Cl}^-$  occupancy factors set to 1.0, the temperature factors of the two symmetry-related anions refined to values of 28.0 and 23.1  $\text{\AA}^2$ , implying that these anion sites are in fact highly occupied.

Besides the increased solvation of the Arg and the new anion-binding site, the other prominent feature of the mutant interface that is apparent in Figure 2 is the movement of the  $\alpha$  chain residues away from the interface. Residues of the  $\alpha$  chain FG corner (Leu 91 $\alpha$ , Arg 92 $\alpha$ , and Val 93 $\alpha$ ), as well as residues of the G helix (Asp 94 $\alpha$ , Pro 95 $\alpha$ , and Val 96 $\alpha$ ) shift away from the interface. The displacements observed for these  $\alpha$  chain residues are greater in magnitude than the displacements observed for residues neighboring the mutation site on the C helix of the  $\beta$  chains. In fact, the shifts observed for the main-chain atoms of Pro 95 $\alpha$  and Val 96 $\alpha$  ( $\sim 0.35$   $\text{\AA}$ ) are the largest differences between the deoxyhemoglobin A and deoxyhemoglobin Rothschild structures (see Figure 6). This shift also alters other interactions at the  $\alpha 1\beta 2$  interface (Figure 3). Specifically, the interaction between Asn 97 $\alpha$  and a water in the switch region of the mutant interface and the loss of the salt bridge between Arg 92 $\alpha$  and Glu 43 $\beta$  can both be attributed to this shift. However, the interaction distances fall just to one side of the 3.5- $\text{\AA}$  cut-off in deoxyhemoglobin A and just to the other side of the 3.5- $\text{\AA}$  cut-off in deoxyhemoglobin Rothschild.

**Analysis of Atomic Displacements: Partitioning between Quaternary and Tertiary Structure Changes.** A mutation in an oligomeric protein can alter both its quaternary and tertiary structures. When the protein is studied in the crystalline state, the mutation can also alter the protein's position in the crystal lattice or even result in a different crystal form. While the Trp  $\rightarrow$  Arg mutation in deoxyhemoglobin Rothschild does not result in a different crystal form (see Table I), it does cause (as described below) structural perturbations that influence all the levels of protein structure, including crystal packing. By superimposing the deoxyhemoglobin Rothschild and deoxyhemoglobin A structures in various ways, it is possible to partition the mutation-induced structural changes into components of tetramer rotation, quaternary structure rearrangement, and deformations of tertiary structure.

As a measure of the mutation-induced perturbations, the vector magnitude of atomic displacements between the native and mutant structures was calculated for all pentapeptides. Specifically, the quantity

$$\delta = \frac{1}{n} \left| \sum_{j=1}^n \Delta \mathbf{r}_j \right|$$

is plotted versus residue number in Figures 5–8, where  $\Delta \mathbf{r}_j$  is the atomic displacement vector for the  $j$ th main-chain atom of a given pentapeptide and  $n$  is the number of backbone atoms ( $=20$  for a pentapeptide). The shift magnitude assigned to the  $i$ th residue corresponds to the value of  $\delta$  for residues  $i - 2$  through  $i + 2$ .

When  $\delta$  is plotted for the  $\alpha$  subunits of the PROLSQ-refined tetramers as they exist in their crystal lattices (i.e., when the tetramers are not superimposed), the two subunits show very different profiles (see Figure 5). The rms value of  $(\delta_{\alpha 2} - \delta_{\alpha 1})$  is 0.069  $\text{\AA}$ . The corresponding  $\delta$  plots for the  $\beta 1$  and  $\beta 2$  subunits also differ from each other (plots not shown) with

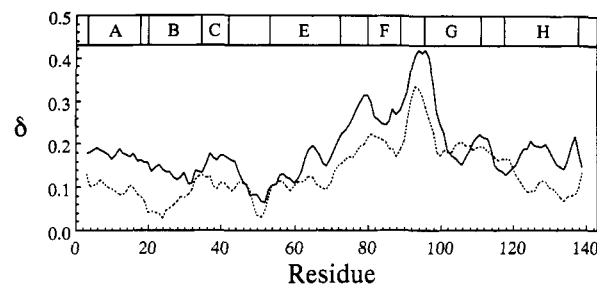


FIGURE 5:  $\delta$  plots (see text) of the PROLSQ-refined  $\alpha 1$  chains (dashed line) and  $\alpha 2$  chains (solid line) before any superposition. The positions of helices A–H are indicated at the top of the plot.

a rms  $(\delta_{\beta 2} - \delta_{\beta 1})$  value of 0.052  $\text{\AA}$ . Essentially the same results were obtained for the XPLOR-refined structures. If this asymmetry is due largely to a rigid-body rotation of the Rothschild tetramer in the crystal lattice, then it should be reduced by a least-squares superposition of the native and mutant tetramers. The  $\delta$  plots in Figure 6 show that this is the case. Figure 6A shows the  $\delta$  profiles for the PROLSQ-refined  $\alpha 1$  and  $\alpha 2$  subunits and the subunit-averaged profile; the corresponding profiles for the XPLOR-refined  $\alpha$  subunits are shown in Figure 6B. Figure 6C shows the overall average  $\delta$  profile obtained by averaging the subunit-averaged PROLSQ and XPLOR  $\delta$  profiles for the  $\alpha$  chains. The analogous  $\beta$  subunit profiles are presented in Figure 6D–F. After the tetramers were superimposed, the rms  $(\delta_{\alpha 2} - \delta_{\alpha 1})$  value dropped to 0.036 and 0.043  $\text{\AA}$  for the PROLSQ- and XPLOR-refined structures, respectively, and the corresponding rms  $(\delta_{\beta 2} - \delta_{\beta 1})$  value dropped to 0.040 and 0.045  $\text{\AA}$ . These rms differences are one measure of the errors in the  $\delta$  magnitudes. Another measure of  $\delta$  magnitude errors is the rms value of the quantity  $(\delta_{\text{PROLSQ}} - \delta_{\text{XPLOR}})$ , which calculates to 0.019  $\text{\AA}$  for the  $\alpha$  subunits and 0.025  $\text{\AA}$  for the  $\beta$  subunits. The average value of the two error estimates is 0.030  $\text{\AA}$  for the  $\alpha$  chains and 0.035  $\text{\AA}$  for the  $\beta$  chains. An overall error estimate of 0.032  $\text{\AA}$  was obtained by averaging the  $\alpha$  and  $\beta$  values.

After removing the contribution of tetramer rigid-body rotation, the  $\delta$  values in Figure 6 are due to the mutation-induced changes in quaternary and tertiary structure. The largest changes are associated with  $\alpha$  chain residues 75 $\alpha$ –100 $\alpha$ , where the  $\delta$  values are 6–12 times the estimated error in  $\delta$ . Interestingly, the  $\delta$  values in the vicinity of the mutation site (34 $\beta$ –44 $\beta$ ) are only 6 times the estimated error in  $\delta$ . The value of  $\delta$  for residues at the FG corner–G helix boundary of the  $\beta$  chains also approaches 6 times the estimated error in  $\delta$ .

By superimposing individual subunits, tertiary structure changes can be isolated from small changes in quaternary structure. The  $\delta$  plots in Figure 7 correspond to those in Figure 6, except that individual subunits were superimposed rather than the entire tetramer. The average error in  $\delta$  in these plots (calculated as described above) is 0.026  $\text{\AA}$  for the  $\alpha$  subunits and 0.031  $\text{\AA}$  for the  $\beta$  subunits, giving an overall estimated error of 0.029  $\text{\AA}$ . Comparison of Figure 7C with Figure 6C shows that the structural changes associated with  $\alpha$  chain residues 90 $\alpha$ –97 $\alpha$  (where the  $\delta$  values are still between 6 and 10 times the estimated error in  $\delta$ ) are for the most part due to a deformation in tertiary structure. In contrast, the structural changes associated with residues 75 $\alpha$ –89 $\alpha$  are reduced to values between 2.5 times and 4.5 times the estimated error in  $\delta$ , indicating that they are largely the result of a small change in quaternary structure. For the  $\beta$  chains, the largest features in Figure 7F, those associated with the C helix and FG corner–G helix boundary, are 4.5 times the estimated error at 33 $\beta$  and 100 $\beta$ , respectively. Since these features in Figure 7F account for the majority of the total  $\delta$  magnitude in the



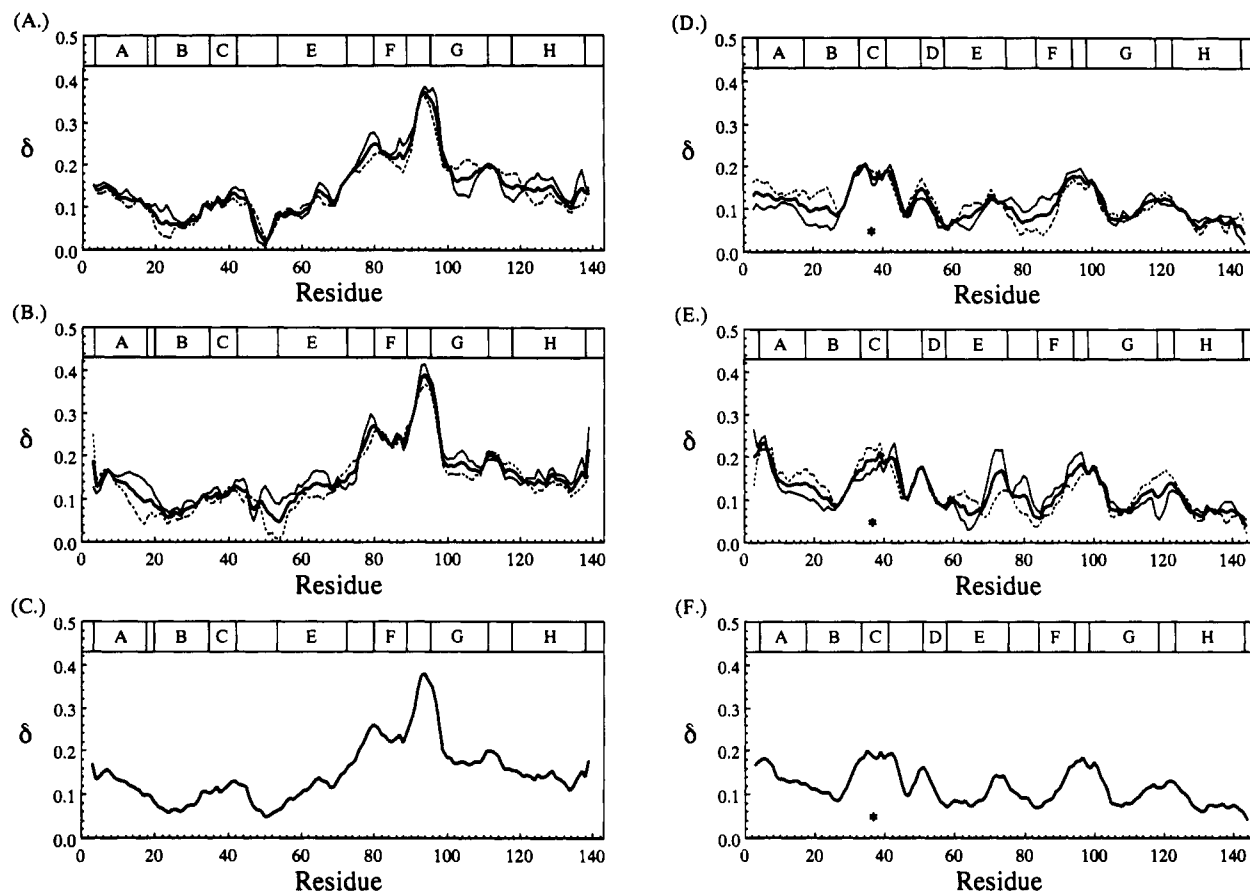


FIGURE 6:  $\delta$  plots for the PROLSQ-refined  $\alpha$  chains (A) and XPLOR-refined  $\alpha$  chains (B) after the native and mutant tetramers have been superimposed. In panels A and B the dashed lines indicate subunit  $\alpha 1$ , the thin solid lines subunit  $\alpha 2$ , and the thick solid lines the average value. The profile in panel C is the overall average of the plots in panels A and B. Profiles in panels D, E, and F are  $\beta$  chain  $\delta$  plots that correspond to the profiles in panels A, B, and C. The asterisk in panels D, E, and F indicates the mutation site ( $37\beta$ ).

corresponding regions of Figure 6F, the small structural changes in the  $\beta$  chains are due mostly to tertiary changes.

The mutation-induced quaternary structure change can be characterized by superimposing one subunit the  $\alpha 1\beta 2$  pair and then calculating a  $\delta$  profile for the other subunit. In Figure 8, the deoxyhemoglobin A and deoxyhemoglobin Rothschild  $\beta 1$  subunits have been superimposed before calculating the  $\delta$  profile for the  $\alpha 2$  subunit. This plot has a minimum at  $42\alpha$ – $44\alpha$ , indicating that the quaternary structural change involves a rotation about an axis that passes through the switch region of the  $\alpha 1\beta 2$  interface. The magnitude of the rotation is approximately  $1^\circ$ .

**Mutation-Induced Changes in Temperature Factors.** Temperature factors were refined for individual atoms using both PROLSQ and XPLOR. For both refinement programs, the main-chain temperature factors for the  $\beta$  chains of deoxyhemoglobin A and deoxyhemoglobin Rothschild did not differ significantly (data not shown). The only significant differences in temperature factors occur at the  $\alpha$  chain COOH-terminal residues (Figure 9). The residues displaying the largest increase in temperature factor, the penultimate Tyr 140 $\alpha$  and carboxy-terminal Arg 141 $\alpha$ , are located in the  $\alpha 1\beta 2$  interface in close proximity to  $37\beta$  and the new anion-binding site (Figure 2). The increase in temperature factor is largest for the carboxyl group of Arg 141 $\alpha$ , which increased by  $14 \text{ \AA}^2$  in the  $\alpha 1$  chain and by  $18 \text{ \AA}^2$  in the  $\alpha 2$  chain during the PROLSQ refinement. Similar differences are observed between the XPLOR refined atomic models. The temperature factor for the N $\epsilon$  atom of Lys 127 $\alpha$ , which forms a salt bridge with the carboxyl group of Arg 141 $\alpha$  on the opposite  $\alpha$  chain, is also increased slightly ( $9 \text{ \AA}^2$  in the  $\alpha 1$  chain and  $5 \text{ \AA}^2$  in the  $\alpha 2$

chain) in the deoxyhemoglobin Rothschild structure.

## DISCUSSION

**Previous Studies.** There have been seven other X-ray studies of mutations at the center of the  $\alpha 1\beta 2$  interface of deoxyhemoglobin (Anderson, 1975; Greer, 1971a,b; Perutz et al., 1988; Pulsinelli, 1973), several of which have reported structural perturbations at large distances from the mutation site. While these studies relied on difference electron density analysis at resolutions between  $5.5$  and  $2.5 \text{ \AA}$ , and none of them included restrained least-squares refinement, they were able to detect and characterize the major mutation-induced structural changes.

Greer (1971b) published  $5.5\text{-\AA}$  difference electron density maps for deoxyhemoglobin Chesapeake,  $92\alpha(\text{FG4}) \text{ Arg} \rightarrow \text{Leu}$ , and deoxyhemoglobin J Capetown,  $92\alpha(\text{FG4}) \text{ Arg} \rightarrow \text{Gln}$ . The only significant features in these difference maps were negative peaks corresponding to the shorter side chains at position  $92\alpha$  in the mutant proteins, implying a high degree of structural isomorphism with native deoxyhemoglobin. In contrast, a  $3.5\text{-\AA}$  difference map of deoxyhemoglobin Yakima (Pulsinelli, 1973),  $99\beta(\text{G1}) \text{ Asp} \rightarrow \text{His}$ , revealed extensive structural changes that included the loss of a critical hydrogen bond with Tyr 42 $\alpha$  at the  $\alpha 1\beta 2$  interface as well as indications of atomic movements at a distance from the mutation site. These long-range changes in structure are probably due to rigid-body subunit movements since the mutation was said to act as "a wedge between the  $\alpha 1$  and  $\beta 2$  subunits, so that they are pushed apart..."

The crystal structure of deoxyhemoglobin Kansas,  $102\beta(\text{G4}) \text{ Asn} \rightarrow \text{Thr}$ , was first analyzed at  $5.5\text{-\AA}$  resolution (Greer,

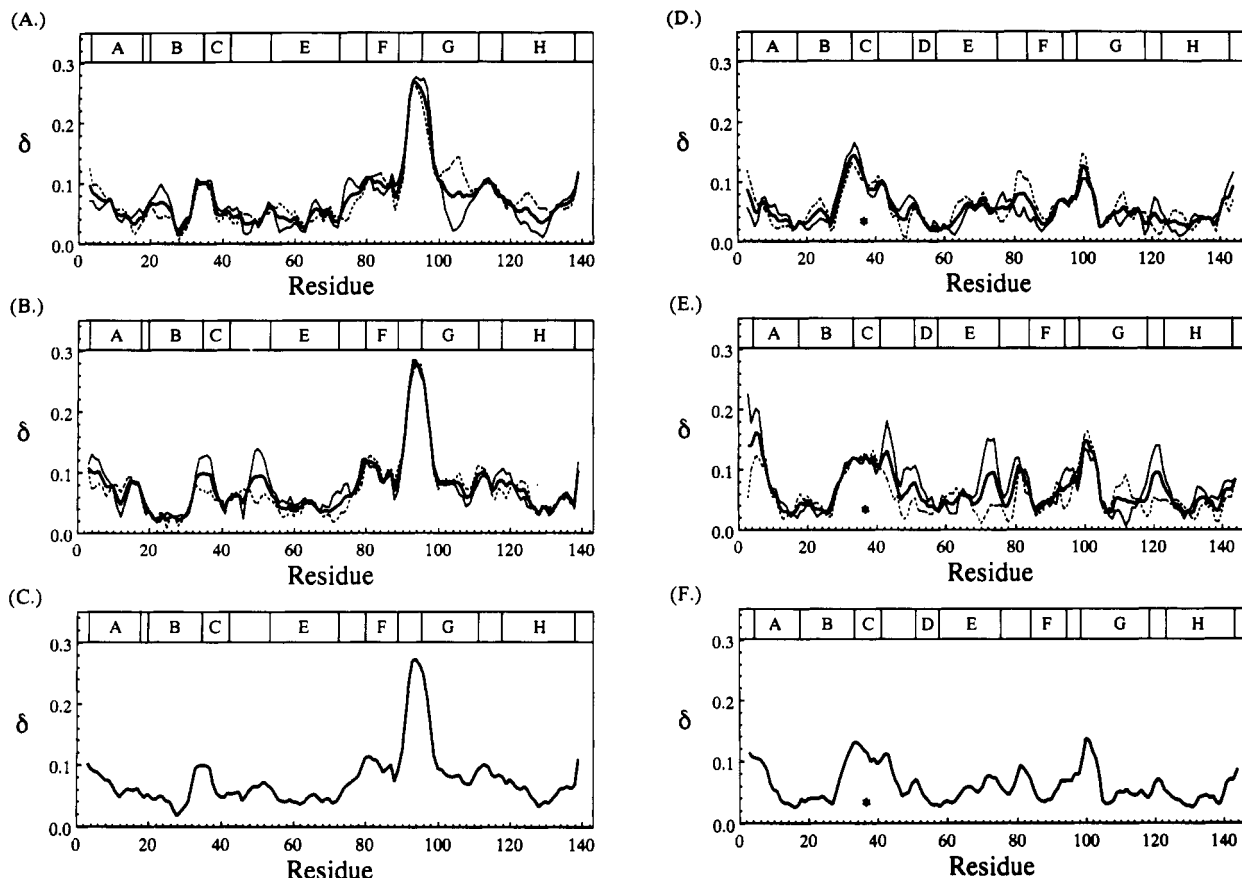


FIGURE 7:  $\delta$  plots for the  $\alpha$  subunits (A, B, and C) and the  $\beta$  subunits (D, E, and F), where tertiary perturbations are isolated by superimposing individual subunits. The profiles are drawn as in Figure 6.

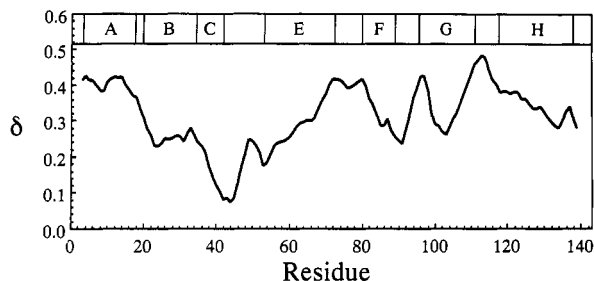


FIGURE 8:  $\delta$  plot for the  $\alpha_2$  subunit of the PROLSQ-refined structures after superimposing the  $\beta_1$  subunit.

1971a) and then at 3.4-Å resolution (Anderson, 1975). The 3.4-Å study revealed structural changes in the vicinity of the mutation site as well as "signs of slight movements throughout the region between  $\alpha$  and  $\beta$  heme pockets". Specifically, these structural changes were interpreted as shifts of the  $\alpha$  chain FG corner and the G and E helices toward the  $\alpha_1\beta_2$  interface as well as shifts of the  $\alpha$  chain C helix and CD corner toward the  $\alpha_1\beta_2$  interface. A related mutation, deoxyhemoglobin Richmond [102 $\beta$ (G4) Asn  $\rightarrow$  Lys] was studied at 5.5-Å resolution and showed similar but more restricted  $\alpha$  chain movements (Greer, 1971a). Movements were also detected in the  $\beta$  subunits of deoxyhemoglobin Kansas, but they appeared to be smaller in magnitude and less extensive. It is unclear how these structural changes are partitioned between shifts of the tetramer in the crystal lattice, and quaternary and tertiary changes, but it is likely that all three types of perturbation contribute to the difference electron density images of deoxyhemoglobin Kansas and deoxyhemoglobin Richmond.

More recently, Perutz et al. (1988) found "unexpectedly large indirect changes in the T structure" as the result a serine for proline substitution in deoxyhemoglobin North Chicago

36 $\beta$ (C2) Pro  $\rightarrow$  Ser, a hemoglobin with high oxygen affinity and low cooperativity. Specifically, a 2.5-Å difference electron density map showed that the mutation causes severe disordering of the  $\alpha$  chain COOH-terminal dipeptide. This rather large structural effect is surprising because Pro 36 $\beta$  interacts with Arg 141 $\alpha$  only weakly through van der Waals contacts that are 3.5 Å or more apart. It is interesting to note that in deoxyhemoglobin Rothschild an increase in the atomic temperature factors for the  $\alpha$  chain COOH-terminal dipeptide also indicates a small degree of disordering for Tyr 140 $\alpha$  and Arg 141 $\alpha$ . This may be the basis for a small increase in ligand affinity in deoxyhemoglobin Rothschild (Sharma et al., 1980).

**Structural Changes in Deoxyhemoglobin Rothschild.** Like the difference Fourier studies of deoxyhemoglobins Yakima and Kansas, direct comparison of the deoxyhemoglobin Rothschild and deoxyhemoglobin A coordinates shows extensive structural changes that extend far beyond the mutation site. However, unlike difference Fourier analysis, comparison of the refined structures allows the structural changes to be resolved into components of tetramer rotation, small changes in quaternary structure, and perturbations in tertiary structure. Initial comparison of the two coordinate sets (Figure 5) indicated that structural changes extended from the mutation site across the  $\alpha_1\beta_2$  interface to the FG corner, continued through the F helix, and reached the EF corner, a distance of over 20 Å. In addition, the mutation-induced perturbations did not display a high degree of symmetry about the dyad axis of the tetramer. Superimposing the deoxyhemoglobin Rothschild and deoxyhemoglobin A tetramers eliminated this asymmetry (see Figure 6) and any contributions to the structural changes that were due to rigid-body movements of the Rothschild tetramer. However, the magnitude and extent of the structural changes remained approximately the same.



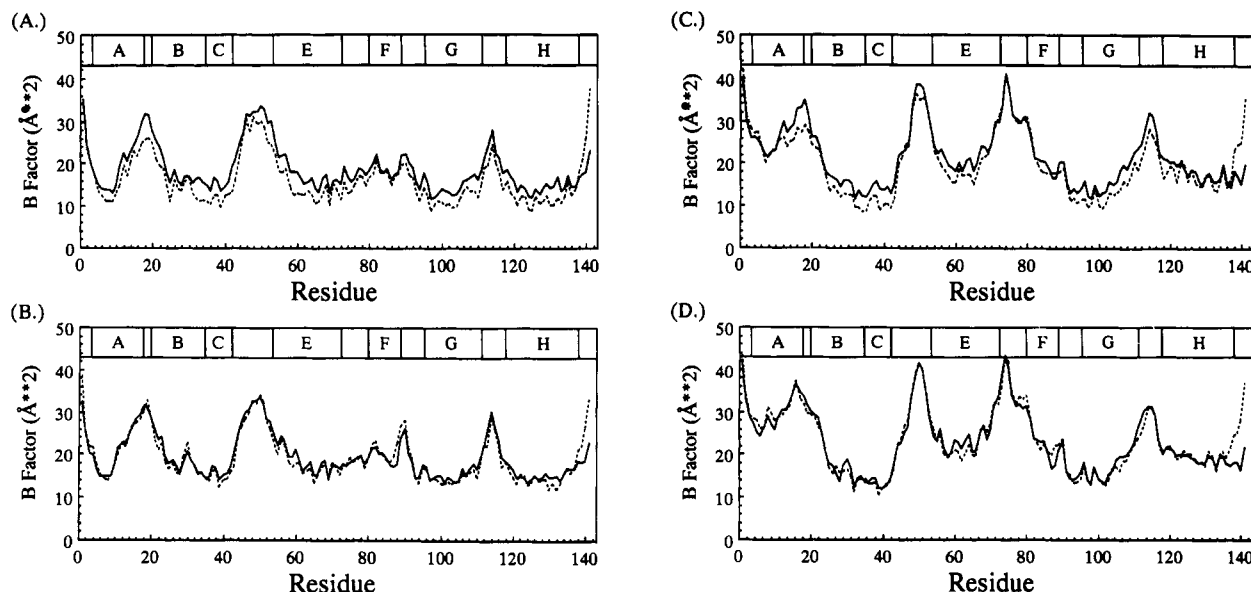


FIGURE 9: Average main-chain isotropic temperature factors are plotted versus residue number for the  $\alpha 1$  (A and B) and  $\alpha 2$  (C and D) subunits of the PROLSQ- (A and C) and XPLOR- (B and D) refined structures of deoxyhemoglobin A (solid lines) and deoxyhemoglobin Rothschild (dashed lines).

By superimposing individual subunits of the native and mutant hemoglobins, the tertiary components of the structural perturbations were isolated from the quaternary structure changes (Figure 7). This analysis showed that the changes in tertiary structure are confined to residues at the  $\alpha 1\beta 2$  interface, with relatively small changes occurring at the mutation site and the largest shifts occurring across the interface from the mutation site in the  $\alpha$  subunit FG corner and the beginning of the G helix. The disruption caused by the Trp  $\rightarrow$  Arg mutation pushes these residues away from the interface and causes the  $\alpha$  subunit to rotate by approximately  $1^\circ$ . The  $\alpha$  subunit pivots about the switch region of the  $\alpha 1\beta 2$  interface (Figure 8), and this appears to cause a secondary perturbation in tertiary structure at the  $\beta$  chain FG corner and the  $\alpha$  chain C helix. What appeared to be long range tertiary structural changes in the  $\alpha$  chain F helix and FG corner are in fact due to the rigid-body rotation of the  $\alpha$  subunit.

Perhaps the most surprising feature of the Rothschild mutation is the creation of a chloride-binding site at the  $\alpha 1\beta 2$  interface. Trp 37 $\beta$  is buried in the hinge region of the  $\alpha 1\beta 2$  interface, where its indole nitrogen forms an intersubunit hydrogen bond with Asp 94 $\alpha$ . When arginine replaces tryptophan at position 37 $\beta$ , the interaction with Asp 94 $\alpha$  is maintained but a hole is produced with the elimination of the six-member ring of the tryptophan side chain. The chloride ion fills this void and provides an additional counterion to maintain local electrical neutrality within the  $\alpha 1\beta 2$  interface.

**Stability of the Hemoglobin Rothschild Tetramer.** In solution, a major difference between hemoglobin Rothschild and hemoglobin A is the decreased stability of the mutant tetramer. Sedimentation and gel filtration studies (Sharma et al., 1980) showed that liganded hemoglobin Rothschild is almost fully dissociated to  $\alpha\beta$  dimers. More recently, Doyle and Ackers (personal communication) have determined accurate equilibrium constants for the dimer-to-tetramer association (in 100 mM Tris-base, 100 mM NaCl, 1 mM Na<sub>2</sub>EDTA, at pH 7.4). In the deoxy form, the free energy of association for hemoglobin A is  $-14.3$  kcal versus  $-12.3$  kcal for hemoglobin Rothschild. In the oxygenated form, the corresponding free energies of association are  $-8.0$  and  $-2.8$  kcal. The 5.2-kcal destabilization of liganded hemoglobin Rothschild is the largest destabilization measured thus far for a mutant hemoglobin

(Doyle and Ackers, personal communication). In an effort to rationalize this large reduction in the stability of the  $\alpha 1\beta 2$  interface, the hemoglobin Rothschild mutation was modeled in the high-resolution structure of human oxyhemoglobin (Shaanan, 1983) using the program TOM/FRODO (Cambillau, 1989). This model-building exercise indicated that the Trp  $\rightarrow$  Arg mutation cannot be accommodated in the  $\alpha 1\beta 2$  interface in a way that allows the arginine side chain to have acceptable conformational angles (Ponder & Richards, 1987), while simultaneously forming an ionic bond with Asp 94 $\alpha$  as it does in the deoxy structure. Also, there does not appear to be sufficient room in the hinge region of the R-state  $\alpha 1\beta 2$  interface to permit the binding of a chloride anion. If this modeling experiment proves to be accurate, the destabilization of the Rothschild R-state  $\alpha 1\beta 2$  interface is the result of burying the side chain of Arg 37 $\beta$  without a counterion.

The structural basis for the 2.0-kcal destabilization of deoxyhemoglobin Rothschild is not obvious from visual inspection of the refined deoxy tetramers. The mutation results mainly in the loss of five noncovalent interactions (one side-chain hydrogen bond, one side-chain van der Waals contact, and three hydrogen bonds associated with a displaced water molecule) and the acquisition of seven new noncovalent contacts (one salt bridge involving two ionic contacts and five hydrogen bonds from two additional bound water molecules). In addition, a void created by the loss of the tryptophan side chain is filled by a chloride anion that makes one ionic bond with the side chain of Arg 37 $\beta$ , a hydrogen bond with the backbone NH of Arg 37 $\beta$ , and several van der Waals contacts. A slight disordering of the  $\alpha$  chain COOH-terminal dipeptide is also a consequence of the mutation. The net difference in the stabilities of the deoxyhemoglobin Rothschild and deoxyhemoglobin A tetramers will depend on the interaction free energies of these interface contacts as well as on the stability of the solvated  $\alpha\beta$  dimers. Recent advances in the use of molecular dynamic simulations to calculate the contributions of individual amino acids to hemoglobin tetramer stability (Gao et al., 1989) may make it possible to evaluate the relative importance of the observed subunit-subunit contacts.

**Chloride-Binding Sites.** The oxygen-linked binding of inorganic anions to human hemoglobin is well known (Imai, 1982). In particular, there is considerable evidence for three

main binding sites per  $\alpha\beta$  dimer. Site 1 is an intrasubunit site located in a pocket between the  $\alpha$ -amino group of Val 1 $\beta$  and the side chain Lys 82 $\beta$  (Arnone, 1972; Nigen & Manning, 1975; Fermi et al., 1984). Site 2 is an intrasubunit site between the  $\alpha$ -amino group of Val 1 $\alpha$  and the  $\beta$ -hydroxyl group of Ser 131 $\alpha$  (Arnone & Williams, 1977; O'Donnell et al., 1979; Fantl et al., 1987). Site 3 is an intersubunit site between the guanidinium group of Arg 141 $\alpha$  and the  $\alpha$ -amino group of Val 1 $\alpha$  of the opposite  $\alpha$  subunit (Chiancone et al., 1975; Nigen et al., 1976; Arnone & Williams, 1977; O'Donnell et al., 1979). While the published crystallographic studies concern the binding of sulfate or phosphate, evidence from solution studies indicates that the same sites bind chloride (O'Donnell et al., 1979; Imai, 1982; Fantl et al., 1987). Since chloride binds to deoxyhemoglobin with dissociation constants between  $10^{-1}$  and  $10^{-2}$  M (Imai, 1982), and since the low-salt crystal form of deoxyhemoglobin used in the present study contains 100 mM chloride, peaks for the electron dense chloride ions should be easily identified in  $F_o - F_c$  Fourier maps. However, despite the fact that the low-salt crystal structures of deoxyhemoglobin A and deoxyhemoglobin Rothschild are now refined to  $R$  values of 0.185 and 0.176 at 1.9- and 2.0-Å resolution, respectively, it has not proved possible to inconclusively model chloride anions at the these three sites.

In an attempt to identify halide-binding sites in the low-salt deoxyhemoglobin A structure, a 2.5-Å difference map was calculated using diffraction data collected on crystals soaked in 300 mM KBr and crystals soaked in 300 mM KCl (unpublished results). This Br<sup>-</sup>-Cl<sup>-</sup> difference electron density map showed a strong peak at site 1 (at 9 times the rms density of the difference map), a dumbbell shaped peak at site 3 (with one lobe at 7 times the rms density of the difference map and the other lobe at 4 times the rms density), and no evidence for the binding of Br<sup>-</sup> to site 2. An analogous 2.5-Å Cl<sup>-</sup>-F<sup>-</sup> difference electron density map showed no clear evidence of the binding of Cl<sup>-</sup> to any of the sites (unpublished results).

The native low-salt deoxyhemoglobin A electron density map does include peaks for solvent molecules in the vicinity of site 1 and site 3, but the locations of Br<sup>-</sup>-Cl<sup>-</sup> difference density peaks and the solvent peaks do not always coincide. Specifically, no solvent molecule can be directly associated with the site 1 Br<sup>-</sup>-Cl<sup>-</sup> difference peak (the nearest solvent molecule is 3.8 Å from the center of this peak). In contrast, there are solvent molecules corresponding to each lobe of the site 3 Br<sup>-</sup>-Cl<sup>-</sup> difference peak. The solvent molecule (modeled as water) in the larger lobe of the site 3 peak has a temperature factor of  $\sim 35$  Å<sup>2</sup>, the one in the smaller lobe has a temperature factor of  $\sim 45$  Å<sup>2</sup>. Because these temperature factors are rather high, it is not possible to differentiate between a water molecule and a low-occupancy chloride ion. The 2.4-Å Br<sup>-</sup>-Cl<sup>-</sup> difference electron density map produced with crystals of deoxyhemoglobin Rothschild soaked in 100 mM Br<sup>-</sup> and crystals grown in 100 mM Cl<sup>-</sup> (see above) showed a very intense peak near the Rothschild mutation site (Figure 4), a weak peak at site 1 (not shown), but no peaks at site 2 or site 3. Taken together, these observations indicate that while Br<sup>-</sup> can bind to site 1 and site 3 in the low-salt crystal form of deoxyhemoglobin, Cl<sup>-</sup> must have a dissociation constant greater than 300 mM in this crystal form, and/or any bound Cl<sup>-</sup> ions must have very high temperature factors.

In view of the difficulty in unambiguously identifying the physiologically important chloride-binding sites in the low-salt crystal structure of deoxyhemoglobin A, the direct visualization of a chloride ion at the hemoglobin Rothschild mutation site was somewhat surprising. The intensity of the electron density

at this site indicates that it is highly occupied at a chloride concentration of 100 mM. Clearly, this mutation-generated anion-binding site has much higher affinity for chloride than do sites 1, 2, and 3. The driving force for binding chloride at this site is the need to have a counterion for the buried side chain of Arg 37 $\beta$ . This structural requirement predicts that the solution properties of hemoglobin Rothschild should be very dependent on chloride concentration. In particular, whereas the dimer-tetramer equilibrium for deoxyhemoglobin A is not sensitive to chloride concentration (Chu & Ackers, 1981), low chloride concentration should favor the formation of  $\alpha\beta$  dimers in deoxyhemoglobin Rothschild.

Recent findings indicate that the oxygen affinity of crystalline deoxyhemoglobin Rothschild is sensitive to chloride concentration. Oxygen binding sites have been carried out directly in low-salt crystals of a recombinant form of hemoglobin Rothschild (Mozzarelli et al., personal communication). The recombinant hemoglobin Rothschild utilized in this study differs from the naturally occurring mutant by the presence of an extra methionine at the NH<sub>2</sub> terminus of each  $\beta$  chain. Mozzarelli et al. have found that the oxygen affinity of the recombinant hemoglobin Rothschild, unlike that of hemoglobin A (Mozzarelli et al., 1991), is sensitive to chloride concentration (personal communication). This indicates that binding of chloride to the mutation-generated anion-binding site modulates the oxygen affinity of the deoxyhemoglobin Rothschild tetramer.

**Ligand Binding Properties.** Hemoglobin Rothschild is unusual in that under some solution conditions (e.g., 0.1 M phosphate buffer, pH 7.8, or 0.1 M bis-Tris chloride buffer, pH 6.8) it has low cooperativity ( $n$  = Hill coefficient  $\sim 1.3$ ) and an oxygen affinity that is the same as the oxygen affinity of hemoglobin A (Sharma et al., 1980). Mutant hemoglobins with very low cooperativity usually have very high oxygen affinities or, in a few cases, low oxygen affinities (Imai, 1982; Bunn & Forget, 1986). Under other solution conditions, the cooperativity of hemoglobin Rothschild remains low while its oxygen affinity varies between one-third and three times that of hemoglobin A (Gacon et al., 1977; Sharma et al., 1980; Doyle and Ackers, personal communication). Thus it has been termed a "high/low affinity hemoglobin mutant" (Sharma et al., 1980). These variations in hemoglobin Rothschild oxygen affinity are probably due to differences in chloride concentration and differences in the ability of phosphate and chloride to serve as a counterion for Arg 37 $\beta$ .

In terms of the allosteric theory of Monod, Wyman, and Changeux (1965), low cooperativity and more or less normal oxygen affinity can be obtained by increasing both the allosteric constant  $L$  ( $= [T]/[R]$  in the absence of ligand) and the parameter  $c$  ( $= K_R/K_T$ , where  $K_R$  and  $K_T$  are the microscopic dissociation constants for the binding of ligand to the R and T states, respectively). Solution measurements are consistent with increased values of  $L$  and  $c$  for hemoglobin Rothschild. Specifically, it is clear from sedimentation (Sharma et al., 1980) and equilibrium measurements (Doyle and Ackers, personal communication) that for hemoglobin Rothschild the liganded R state is destabilized much more than the unliganded T state. If the same is true for the unliganded R state versus the unliganded T state, then  $L$  should increase by about two orders of magnitude. Kinetic measurements (Sharma et al., 1980) indicate that deoxyhemoglobin Rothschild has increased ligand affinity compared to deoxyhemoglobin A, implying the  $c$  should be larger for hemoglobin Rothschild. The structural basis for an increased value of  $L$  appears to be the inability of the R-state interface to provide

counterions for Arg 37 $\beta$ , and the increased oxygen affinity of the T state may be due in part to the disordering of the  $\alpha$  subunit COOH-terminal dipeptide.

## ACKNOWLEDGMENTS

We thank Helen Ranney for providing whole blood containing hemoglobin Rothschild. We thank Gary Ackers, Mike Doyle, and co-workers for providing purified hemoglobin Rothschild and data prior to publication. We gratefully acknowledge the use of the data collection facilities and the expertise at The University of California at San Diego Resource for Protein Crystallography. We thank David Mitchell for help with the halide soak experiments, and we thank Gloria Borgstahl and Jeff Regan for programs used to identify solvent molecules. We also thank Drs. Mozzarelli, Rivetti, Noble, Henry, Eaton, and Rossi for providing unpublished data on oxygen-binding studies of crystalline hemoglobin Rothschild.

Registry No. Cl<sup>-</sup>, 16887-00-6; O<sub>2</sub>, 7782-44-7; deoxyhemoglobin Rothschild, 65278-15-1.

## REFERENCES

- Anderson, L. (1975) *J. Mol. Biol.* **94**, 33-49.
- Arnone, A. (1972) *Nature* **237**, 146-149.
- Arnone, A., & Williams, D. L., Jr. (1977) in *Molecular Interaction of Hemoglobin* (Labie, D., Poyart, C., & Rosa, J., Eds.) pp 15-22, Institut National de la Santé et de la Recherche Médicale, Paris.
- Arnone, A., Rogers, P. H., & Briley, P. D. (1980) in *Biophysics and Physiology of Carbon Dioxide* (Bauer, C., Gros, G., & Bartels, H., Eds.) pp 67-74, Springer-Verlag, Berlin.
- Baldwin, J., & Chothia, C. (1979) *J. Mol. Biol.* **129**, 175-220.
- Bunn, H. F., & Forget, B. G. (1986) *Hemoglobin—Molecular, Genetic, and Clinical Aspects*, W. B. Saunders Co., Philadelphia.
- Brünger, A., Kuriyan, J., & Karplus, M. (1987) *Science* **235**, 458-460.
- Cambillau, C. (1989) in *Silicon Graphics Geometry Partners Directory*, spring volume, pp 61, Silicon Graphics, Mountain View, CA.
- Chu, A. H., & Ackers, G. K. (1981) *J. Biol. Chem.* **256**, 1199-1205.
- Chiancone, E., Norne, J. E., Forsén, S., Bonaventura, J., Brunori, M., Antonini, E., & Wyman, J. (1975) *Eur. J. Biochem.* **55**, 385-390.
- Fantl, W. J., DiDonato, A., Manning, J. M., Rogers, P. H., & Arnone, A. (1987) *J. Biol. Chem.* **262**, 12700-12713.
- Fermi, G., Perutz, M. F., Shaanan, B., & Fourme, R. (1984) *J. Mol. Biol.* **175**, 159-174.
- Gacon, G., Belkhdja, O., Wajcman, H., & Labie, D. (1977) *FEBS Lett.* **82**, 243-246.
- Gao, J., Kuczera, K., Tidor, B., & Karplus, M. (1989) *Science* **244**, 1069-1072.
- Gelin, B. R., & Karplus, M. (1977) *Proc. Natl. Acad. Sci. U.S.A.* **74**, 801-805.
- Gelin, B. R., Lee, A. W.-M., & Karplus, M. (1983) *J. Mol. Biol.* **171**, 489-559.
- Greer, J. (1971a) *J. Mol. Biol.* **59**, 99-105.
- Greer, J. (1971b) *J. Mol. Biol.* **62**, 241-249.
- Hendrickson, W. A. (1985) *Methods Enzymol.* **115**, 252-270.
- Howard, A. J., Nielsen, C., & Xuong, N. H. (1985) *Methods Enzymol.* **114**, 452-472.
- Imai, K. (1982) *Allosteric Effects in Haemoglobin*, Cambridge University Press, Cambridge.
- Ip, S. H. C., & Ackers, G. K. (1971) *J. Biol. Chem.* **252**, 82-87.
- Jones, T. A. (1985) *Methods Enzymol.* **115**, 157-171.
- Kabsch, W. (1976) *Acta Crystallogr.* **A32**, 922-923.
- Kuriyan, J., Wilz, S., Karplus, M., & Petsko, G. A. (1986) *J. Mol. Biol.* **192**, 133-154.
- Monod, J., Wyman, J., & Changeux, J. P. (1965) *J. Mol. Biol.* **12**, 88-118.
- Mozzarelli, A., Rivetti, C., Rossi, G. L., Henry, E. R., & Eaton, W. A. (1991) *Nature* **351**, 416-419.
- Nigen, A. M., & Manning, J. M. (1975) *J. Biol. Chem.* **250**, 8248-8250.
- Nigen, A. M., Bass, B. D., & Manning, J. M. (1976) *J. Biol. Chem.* **251**, 7638-7643.
- O'Donnell, S., Mandaro, R., Schuster, T. M., & Arnone, A. (1979) *J. Biol. Chem.* **254**, 12204-12208.
- Perutz, M. F. (1968) *J. Cryst. Growth* **2**, 54-56.
- Perutz, M. F. (1970) *Nature* **228**, 726-734.
- Perutz, M. F., Fermi, G., Fogg, J., & Rahbar, S. (1988) *J. Mol. Biol.* **201**, 459-461.
- Pettigrew, D. W., Romeo, P. H., Tsapis, A., Thillet, J., Smith, M. L., Turner, B. W., & Ackers, G. K. (1982) *Proc. Natl. Acad. Sci. U.S.A.* **79**, 1849-1853.
- Ponder, J. W., & Richards, F. M. (1987) *J. Mol. Biol.* **193**, 775-791.
- Pulsinelli, P. D. (1973) *J. Mol. Biol.* **74**, 57-66.
- Shaanan, B. (1983) *J. Mol. Biol.* **171**, 31-59.
- Sharma, V. S., Newton, G. L., Ranney, H. M., Ahmed, F., Harris, J. W., & Danish, E. H. (1980) *J. Mol. Biol.* **144**, 267-280.
- Valdes, R., & Ackers, G. K. (1977) *J. Biol. Chem.* **252**, 88-91.
- Ward, K. B., Wishner, B. C., Lattman, E. E., & Love, W. E. (1975) *J. Mol. Biol.* **98**, 237-256.